NASA Technical Paper 2900

AVSCOM Technical Report 88-C-008

1989

Determination of Combustion Gas Temperatures by Infrared Radiometry in Sooting and Nonsooting Flames

Valerie J. Lyons
Lewis Research Center
Cleveland, Ohio

Carmen M. Gracia-Salcedo
Propulsion Directorate
USAARTA-AVSCOM
Lewis Research Center
Cleveland, Ohio

NASA
National Aeronautics and Space Administration
Office of Management
Scientific and Technical Information Division

Summary

Flame temperatures in nonsooting and sooting environments were successfully measured by radiometry for premixed propane-oxygen laminar flames stabilized on a water-cooled, porous sintered-bronze burner. The measured temperatures in the nonsooting flames were compared with fine-wire thermocouple measurements. The results show excellent agreement below 1700 K, and when the thermocouple measurements were corrected for radiation effects, the agreement was good for even higher temperatures. The benefits of radiometry are (1) the flow is not disturbed by an intruding probe, (2) calibration is easily done by using a blackbody source, and (3) measurements can be made even with soot present. The theory involved in the radiometry measurements is discussed, as well as the energy balance calculations used to correct the thermocouple temperature measurements.

Introduction

Combustion gas temperatures are difficult to measure since radiation losses caused by the high temperatures associated with flames produce errors in the thermocouple readings. Temperature measurements are also limited by the thermocouple material. In addition, a special problem arises in measuring combustion gas temperatures when soot is present. The soot quickly builds up on the thermocouple, continuously changing the emissivity of the thermocouple, which makes radiation heat transfer corrections very difficult.

Engine designers are interested in soot research since the presence of soot increases the radiation heat transfer to engine walls, reducing engine life. Interest in soot formation in flames led to a desire to nonintrusively determine the soot volume fractions, particle sizes, and number densities using laser scattering-extinction in both diffusion (refs. 1 and 2) and premixed (refs. 3 and 4) flames. Local gas temperature also is an important factor in the production of soot. To further understand the soot formation and burnup processes, it is necessary to measure the temperatures in flames and in the combustion gases downstream of the flame fronts. A viable measurement technique is infrared radiometry. This method is nonintrusive and does not require seeding the flow with any foreign particles or chemicals. The infrared monochromatic radiation method of gas pyrometry was first developed by Schmidt (ref. 5) in 1909. Much later, this technique was used as the basis for the modern, commercial infrared radiometer which was used in this study.

This investigation determined temperature profiles in both nonsooting and sooting premixed propane-oxygen laminar flames. Infrared radiometry was used, and the results in the nonsooting flames were compared to fine-wire thermocouple measurements. The premixed flames were stabilized on a water-cooled, porous sintered-bronze burner (fig. 1). This burner produced a very uniform flow field in which the equivalence ratio and cold gas velocity could be varied with precise micrometer valves. This type of burner has been used in many research programs (refs. 6 to 10).

Theory

The laws of radiation originated by Stefan-Boltzmann, Wien, Planck, and others establish definite and precise relationships between an object's temperature and composition and the radiation it emits. Conversely, by making accurate spectral measurements of the radiation received from a remote object, much can be learned about its thermal history and composition (ref. 11). These spectral measurements are made by using radiometry. The conventional process of radiometric data interpretation uses the basic laws of radiation together with the detailed characteristics of the optical, electronic, and detector elements of the instrument.

One approach treats the radiometer as a system which has a transfer function, or response factor, K_s, which converts the radiometer output voltage and scale settings to an absolute radiation measurement. The radiometer system response factor is defined as (ref. 12)

$$K_s = \frac{SV}{N_T - N_r} \tag{1}$$

where

S instrument electronic attenuation factor

V recorded output voltage

N_T effective radiance, W/cm^2-sr

N_r effective radiance of radiometer internal reference, from calibration, W/cm^2-sr

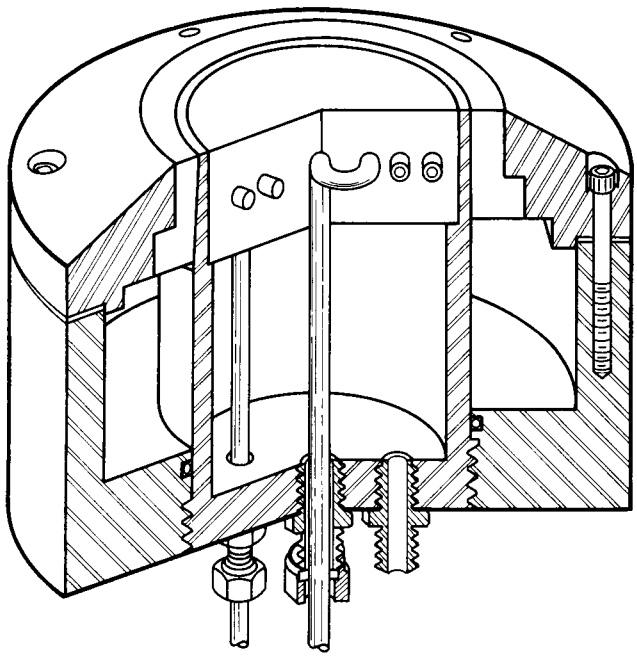

Figure 1.—Cross section of flat flame burner.

(A complete list of symbols is provided in appendix A for the reader's convenience.) First, N_T must be determined by using a graphical technique along with the calibration data for the radiometer; N_T is defined as

$$N_T = \int_{\lambda_1}^{\lambda_2} R_\lambda N_\lambda \, d\lambda \tag{2}$$

where

R_λ normalized product of detector response and optical filter transmission characteristics (provided by instrument calibration)

N_λ blackbody spectral radiance at selected temperature given by Planck's equation:

$$N_\lambda = \frac{C_1}{\lambda^5}\left[\frac{1}{e^{C_2/\lambda T}-1}\right] \tag{3}$$

where

C_1 first radiation constant, 1.19×10^4 W-μm/sr-cm^2

C_2 second radiation constant, 1.438×10^4 μm-K

T blackbody temperature, K

λ all wavelengths in range of detector and filter (from λ_1 to λ_2)

In order to determine R_λ, the radiometer detector must be calibrated over a range of wavelengths, and the detector response must be normalized and plotted versus wavelength (fig. 2). Then the optical filter must be calibrated in a similar fashion to produce a normalized calibration curve as shown in figure 3. The values of the detector response and the filter response at a given wavelength are multiplied together, and the resulting curve is again normalized. This new curve is R_λ, which is used in equation (2) along with equation (3) to determine N_T.

Evaluating the integral in equation (2) for a selected temperature will give its corresponding value of N_T. These results were tabulated so that in the future, when an experimental value of N_T is found, the table will provide the corresponding temperature (ref. 12). For instance, the table is immediately useful to determine N_r for equation (1). The internal reference temperature was measured at the time of calibration. We now use the radiance versus temperature (N_T versus T) table to look up this reference temperature and find N_r.

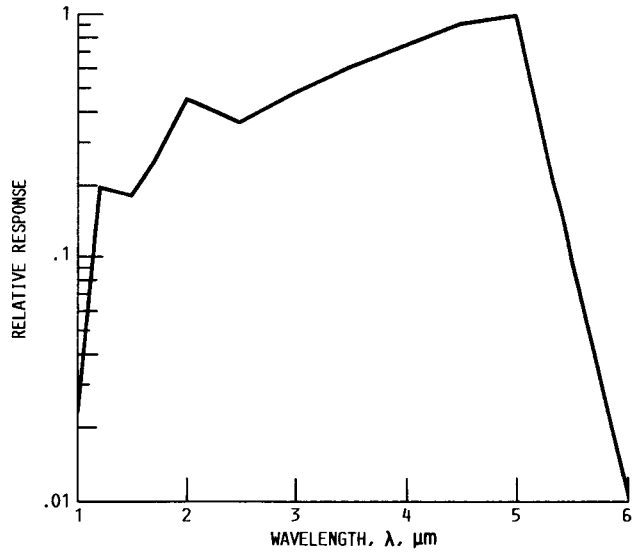

Figure 2.—Radiometer detector response.

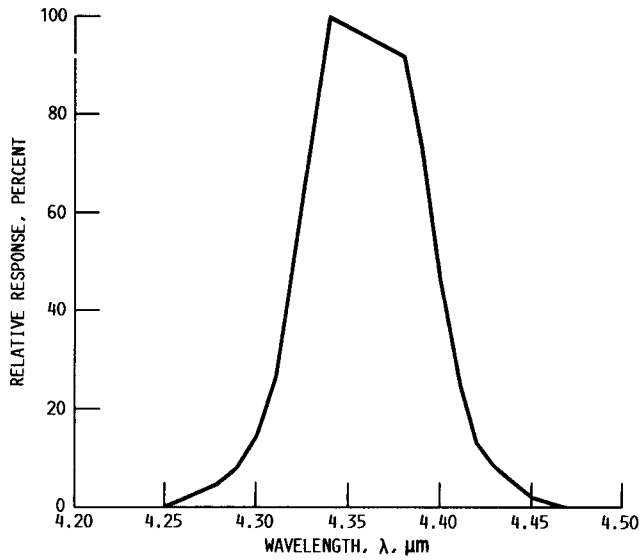

Figure 3.—Radiometer filter response.

After using a blackbody source to supply a known temperature to calibrate our system and determine K_s, we can proceed to determine unknown temperatures by using equation (1) rearranged as

$$N_T = N_r + \frac{SV}{K_s} \tag{4}$$

Experimental Method

When attempting to measure a flame temperature, we cannot assume that the flame is a blackbody (emissivity = 1). The flame emissivity must be determined experimentally. Neglecting the effects of the surrounding atmosphere and assuming the flame is at a uniform temperature, we seek the flame spectral emittance $\epsilon_{\lambda 1 f}$ at λ_1, which is chosen to be 4.4 μm for our study in order to collect CO_2 radiation, since CO_2 is plentiful in combustion products. The following identity will be used:

$$\alpha_{\lambda 1 f} = \epsilon_{\lambda 1 f}$$

where

$\alpha_{\lambda 1 f}$ spectral absorptance of the flame

$\epsilon_{\lambda 1 f}$ spectral emittance of the flame

and we can define $\tau_{\lambda 1 f}$ to be the spectral transmittance, such that $1 = \alpha + \tau$.

Since the voltage measured by the radiometer is a measure of the radiation intensity, voltages and radiation intensity will be considered to be interchangeable in the following analysis. The method (ref. 5) requires measurement of four voltages (fig. 4):

V_o voltage with blackbody covered with shutter

V_{bb} voltage with blackbody radiation only

V_{f1} voltage with flame radiation only

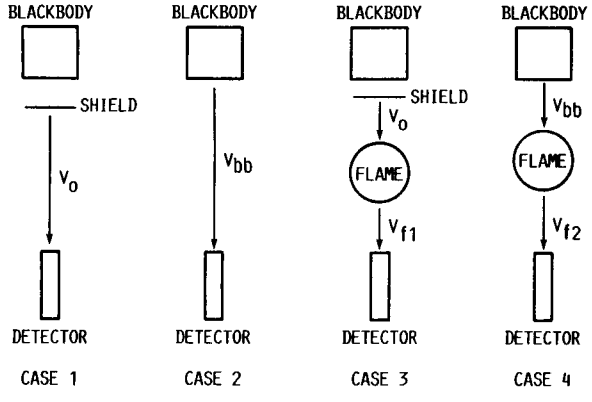

Figure 4.—Required voltage readings for radiometer flame temperature measurement.

V_{f2} voltage with flame plus transmitted blackbody radiation

Two equations can be written for cases 3 and 4 seen in figure 4:

$$V_{f1} = V_o \tau_{\lambda 1 f} + \alpha_{\lambda 1 f} V_{\lambda 1 bf} \tag{5}$$

and

$$V_{f2} = V_{bb} \tau_{\lambda 1 f} + \alpha_{\lambda 1 f} V_{\lambda 1 bf} \tag{6}$$

where $V_{\lambda 1 bf}$ is the voltage that would be recorded if the flame were a blackbody. Since the flame is not a blackbody, this voltage (radiation intensity) must be multiplied by the flame absorptance in these equations.

Subtraction of equations (5) and (6) yields

$$V_{f2} - V_{f1} = \tau_{\lambda 1 f}(V_{bb} - V_o)$$

which can be solved for the flame transmittance,

$$\tau_{\lambda 1 f} = \frac{V_{f2} - V_{f1}}{V_{bb} - V_o} \tag{7}$$

Now, either equation (5) or (6) can be used to find $V_{\lambda 1 bf}$, the voltage that would be measured if the flame were a blackbody source radiating at the flame temperature. For example, using equation (5) yields

$$V_{\lambda 1 bf} = \frac{V_{f1} - V_o \tau_{\lambda 1 f}}{\alpha_{\lambda 1 f}}$$

which, upon using $\alpha = 1 - \tau$, becomes

$$V_{\lambda 1 bf} = \frac{V_{f1} - V_o \tau_{\lambda 1 f}}{1 - \tau_{\lambda 1 f}} \tag{8}$$

By returning to the radiometer equation (4) and using the voltage $V_{\lambda 1 bf}$ which corrects the flame to a "black" flame, a value for N_T is determined which is the effective flame radiance corrected for flame emittance.

$$N_T = N_r + \frac{S V_{\lambda 1 bf}}{K_s} \tag{9}$$

By using this N_T, the corresponding flame temperature is found from the table. A curve fit to this table is used in a computer program for calculating a temperature from the four measured voltages. This program is shown in appendix B. It

is written in the APL language and can be run on IBM-PC/AT or compatible using the APL*Plus System (ref. 13).

With this method, if there is soot in the flame, the soot will radiate in the 4.4-μm wavelength along with the CO_2. It is unnecessary to differentiate between the radiation from the soot and the radiation from the CO_2, however, because the CO_2 and soot are approximately at the flame temperature. The radiometer receives the radiation from both and converts it to the flame temperature. Of course, the flame emissivity will be different when there is soot, but the emissivity is measured and used in the calculations when determining the flame temperature.

Thermocouple Temperature Measurements

An energy balance between the convection to and the net radiation away from the spherical thermocouple bead is required to extract the true gas temperature from the bead temperature reading. Because the leads are aligned along an isotherm, we assume that there is no conduction down the leads. Figure 5(a) shows a photograph of the thermocouple apparatus. The upper wire is platinum/platinum-rhodium for flame temperature measurements, and the lower wire (Chromel/Alumel) can more accurately determine the lower temperatures of the burner surface (near 800 K). Figure 5(b) shows the position of the thermocouple bead in the flame.

The convective heat transfer coefficient is approximated by using Nusselt number *Nu* correlations, where for a sphere in the creeping flow regime (i.e., Reynolds number *Re* approaching zero) (ref. 14)

$$Nu = \frac{hD}{k} = 2 + 0.37Re^{0.6}Pr^{0.33} \tag{10}$$

for all Reynolds and Prandtl *Pr* numbers of interest in the flat flame flow field. Here *h* is the average heat transfer coefficient

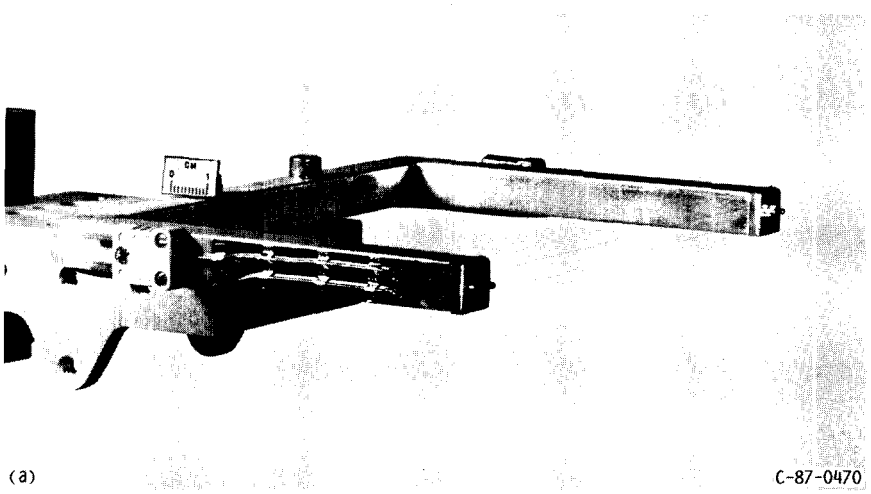

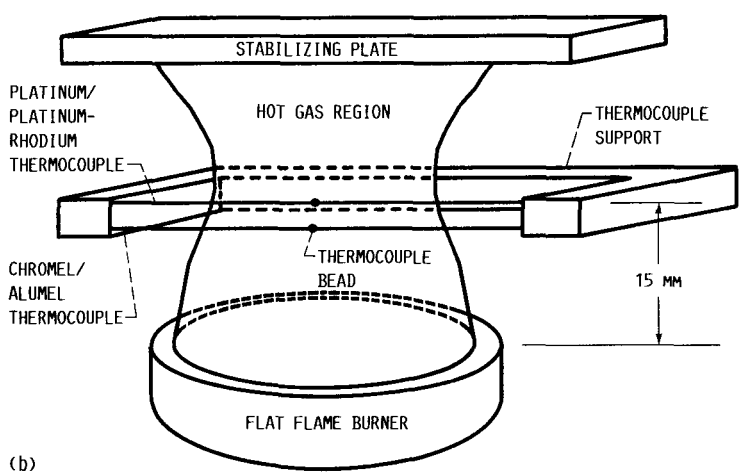

(a) Thermocouple apparatus.
(b) Location of thermocouple in flame.

Figure 5.—Thermocouple used in flame temperature measurements.

(W/m^2-K), D is the bead diameter (m), and k is the gas thermal conductivity (W/m-K). For the propane-oxygen flame (assuming only water and carbon dioxide products), for 1 mole of propane, 4 moles of CO_2 and 3 moles of H_2O are formed. The thermal conductivities of CO_2 and H_2O are formed as a function of temperature (ref. 15), and then the thermal conductivity for the mixture can be calculated as

$$k = \frac{4}{7} k_{CO_2} + \frac{3}{7} k_{H_2O}$$

An energy balance is then made around the thermocouple bead by using an optically thin approximation, where the gas and soot particles emit but do not attenuate radiation. Radiation is exchanged between the bead and the burner surface, the upper stabilizing plate, the hot gases, the soot, and the ambient atmosphere. Surfaces are assumed to be in local thermal equilibrium, diffuse and gray, however, the ambient atmosphere is assumed to be black. The net radiation flux q_r'' out of the bead is then

$$q_r'' = \epsilon_b \sigma T^4 - \alpha_b F_{bp} \epsilon_p \sigma T_p^4 - \alpha_b F_{bB} \epsilon_B \sigma T_B^4 - \alpha_b F_{bs} \epsilon_s \sigma T_s^4 - a_b F_{bg} \epsilon_g \sigma T_g^4 - \alpha_b F_{b\infty} \sigma T_\infty^4 \qquad (11)$$

where the subscripts indicate—b, bead; p, upper plate; B, burner surface; s, soot; g, gas; and ∞, ambient; and where ϵ is the emissivity, σ is the Stefan-Boltzmann constant, α is the absorptivity, and F_{ij} are view factors.

Kirchhoff's law and the gray assumption are used to substitute the emissivity ϵ_b for the absorptivity α_b of the bead. This emissivity is found as a function of temperature from (ref. 16).

$$\epsilon_b = 1.507 \times 10^{-4}(T_b) - 1.596 \times 10^{-8}\left(T_b^2\right) \qquad (12)$$

for $0 < T_b < 2230$ K.

The emissivities of the steel plate and bronze burner surface are approximately (ref. 17) $\epsilon_p \approx 0.3$ and $\epsilon_B \approx 0.1$. The emissivity of the gases are found from

$$\epsilon_g = \epsilon_{CO_2} + \epsilon_{H_2O} - \Delta\epsilon \qquad (13)$$

where the ϵ of each of the gases is dependent on the partial pressure and the path length through the gas from the bead. Figures showing the emissivities for carbon dioxide and for water vapor are found in Siegel and Howell (ref. 17). The $\Delta\epsilon$, which corrects for the spectral overlap of the absorption bands of CO_2 and H_2O, was found to be negligible for this small flame (a path length of 15 mm). Then, $\epsilon_g = 0.025 + 0.0095 = 0.0345$.

The shape factors were determined by using a model (ref. 17) of a sphere (the thermocouple bead was nearly spherical) over a circular plate (with a radius of 3 cm), giving $F_{bp} = F_{bB} = 0.276$; then $F_{b\infty} = 1 - F_{bp} - F_{bB} = 0.448$, while the gas surrounding the bead gives $F_{bg} = 1$. There was no soot present in the flame for the thermocouple measurements. This reduces equation (11) to

$$q_r'' = \epsilon_b \sigma \left[T_b^4 - 0.0828 T_p^4 - 0.0276 T_B^4 - 0.0345 T_g^4 - 0.448 T_\infty^4 \right]$$

This radiative heat transfer is balanced by the convective heat transfer $q_c'' = h(T_g - T_b) = h\Delta T = q_r''$, so the gas temperature is found from

$$T_g = T_b + \frac{\epsilon_b \sigma}{h} \left[T_b^4 - 0.0828 T_p^4 - 0.0276 T_B^4 - 0.0345 T_g^4 - 0.448 T_\infty^4 \right] \qquad (14)$$

Iteration is required since the gas conductivity is a function of temperature and this equation includes a fourth power term in T_g. For example, for a thermocouple reading of 1780 K, the burner surface was nearly 800 K, the plate was approximately 1000 K, and the gas temperature was

$$T_g = 1780 + 58 - 0.47 - 0.07 - 2.42 - 0.02 = 1835 \text{ K}$$

This shows that the major contributions to the thermocouple correction come from the radiation loss from the bead and from the additional radiation from the hot flame gases. The contributions from the burner surface, the plate, and the ambient atmosphere were negligible. An error analysis of this method (ref. 14) showed that, in a nonsooting flame, ΔT ($= T_g - T_b$) was ± 15 percent accurate with the errors in T_b and T_g both approximately ± 3 percent.

Results

The flame temperature measured 15 mm above the burner surface and determined by the radiometer is shown as a function of equivalence ratio in figure 6, for three cold gas velocities—6, 9, and 12 cm/s. These flames were nonsooting so that they could be compared with fine-wire (0.08-mm-diameter) platinum/platinum-rhodium thermocouples. For the higher flow rates (9 and 12 cm/s), there is an increase in temperature with an increase in equivalence ratio until the ratio is nearly stoichiometric. The temperature dips near the stoichiometric equivalence ratio, then continues to climb until near an equivalence ratio of 1.3, where the temperature begins to drop again. This is not the trend for adiabatic well-stirred reactor combustion of propane-oxygen mixtures as a function of equivalence ratio.

Figure 7(a) shows the expected temperature profile predicted by equilibrium chemical kinetics calculations (ref. 18). Notice

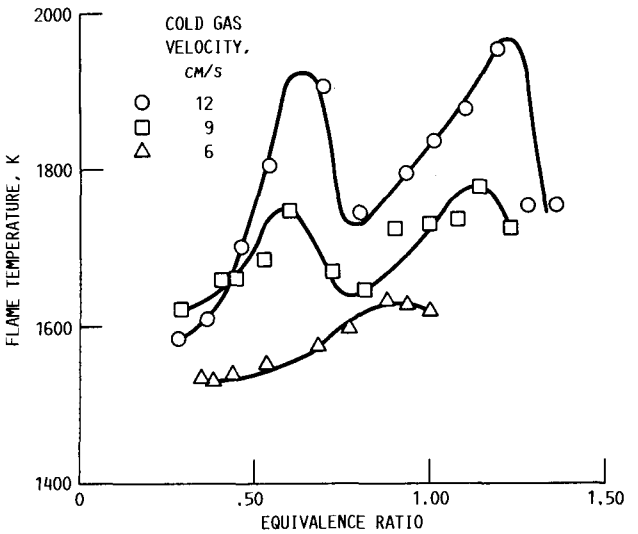

Figure 6.—Flame temperature determined by radiometry.

the peak in temperature near the stoichiometric equivalence ratio. Figure 7(b) is a plot of the laminar flame velocities as a function of equivalence ratio for propane-air flames (ref. 19). The peak velocity is also seen to occur near the stoichiometric equivalence ratio. The velocity will be much higher when pure oxygen is used instead of air, as shown in the relative plot of maximum flame velocities as a function of mole fraction of oxygen shown in figure 7(c) (ref. 20). So, both the velocity and temperature profiles are expected to peak near the stoichiometric equivalence ratio. This can be used to explain the dip in flame temperature near the stoichiometric equivalence ratio for the flat flame burner. The flame speed increases with increasing equivalence ratio, and the flame begins to nestle closer to the water-cooled (i.e., nonadiabatic) burner surface, losing heat to the burner. Since the flame speed is maximum at the stoichiometric equivalence ratio, the greatest heat loss to the burner is seen here, even though the flame temperature should be the highest. Above the stoichiometric equivalence ratio, the flame speed begins to decrease, allowing the flame to lift farther from the burner surface, causing it to lose less heat to the water-cooled burner. This lessening of the heat transfer to the burner overcomes the lowering of the flame temperature due to the equivalence ratio. This effect is seen as an overall increase in the flame temperature until the equivalence ratio effect predominates when the flame has reached a position far enough away from the burner to be essentially adiabatic. At this point (near an equivalence ratio of 1.3), the temperature begins to drop with an increase in equivalence ratio as expected.

The low flow rate case (6 cm/s) has a flow velocity that allows the flame to remain at nearly the same position for all equivalence ratios. The temperature increases with increasing equivalence ratio to near the stoichiometric equivalence ratio and decreases thereafter as predicted by well-stirred reactor calculations.

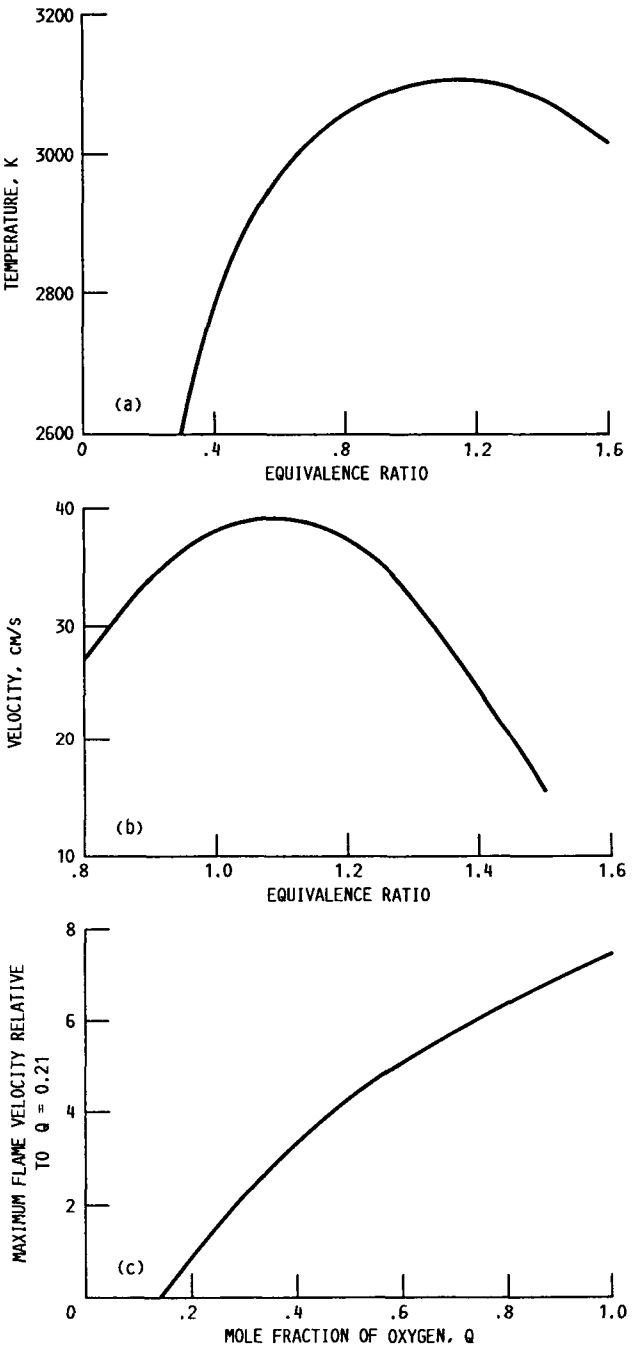

(a) Equilibrium flame temperatures for propane-oxygen premixed flames.
(b) Laminar burning velocity as function of equivalence ratio for propane-air flames.
(c) Effect of oxygen concentration on relative flame velocities using propane fuel.

Figure 7.—Predicted flame temperatures and laminar burning velocities for adiabatic, premixed flames. Initial mixture temperature, 298 K; all flames at 1 atm.

Figure 8 shows a comparison of fine-wire thermocouple readings with the radiometer temperature measurements of figure 6. The 45° line shows where perfect agreement would

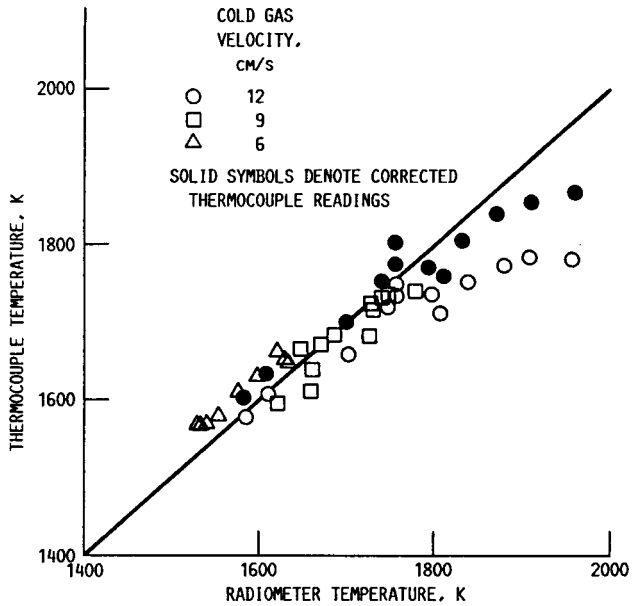

Figure 8.—Comparison of radiometer and thermocouple temperature measurements.

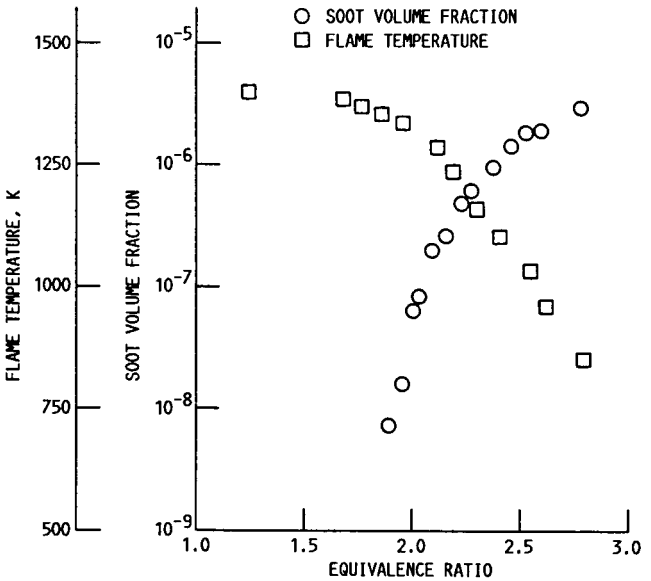

Figure 9.—Soot volume fractions and flame temperatures as functions of equivalence ratio. Height above burner, 15 mm; cold gas velocity, 3.5 cm/s.

occur. The two techniques agree very well for temperatures below 1700 K. Above this temperature, radiation losses from the thermocouple begin to have a greater effect and the thermocouple reads a lower temperature. The thermocouple readings for the 12 cm/s case were corrected, and the corrected results are seen as solid symbols in figure 8.

The radiometer was then used to measure temperature in a sooting flame ($\phi > 1.7$) as a function of equivalence ratio ϕ, for a cold gas velocity of 3.4 cm/s, 15 mm above the burner. This temperature is shown in figure 9 along with the soot volume fraction (fraction of flame volume filled by the soot particles in parts per million) measured by a scattering-extinction laser diagnostic technique (ref. 4) for the same flame. As expected, the flame temperature decreases with increasing equivalence ratio, for equivalence ratios over 1.0, partially due to the increase in soot particles radiating heat to the environment.

Conclusions

Flame temperatures in both nonsooting and sooting environments have been successfully measured by radiometry. In the nonsooting flames, comparisons with fine-wire thermocouples showed excellent agreement below 1700 K, and when the thermocouples were corrected for radiation effects, the agreement was good for even higher temperatures. The benefits of radiometry are (1) the flow is not disturbed by an intruding probe, (2) calibration is easily done by using a blackbody source, and (3) measurements can be made even with soot present.

Lewis Research Center
National Aeronautics and Space Administration
Cleveland, Ohio, November 28, 1988

Appendix A
Symbols

C_1, C_2	first and second radiation constants, respectively
D	bead diameter
F_{ij}	view factors
h	average heat transfer coefficient
K_s	transfer function (or response factor)
k	gas thermal conductivity
N_r	effective radiance of radiometer internal reference (from calibration)
N_T	total effective radiance
N_λ	blackbody spectral radiance at selected temperature
Nu	Nusselt number
Pr	Prandtl number
q_c''	convective heat transfer
q_r''	radiative heat transfer
R_λ	normalized product of detector response and optical filter transmission
Re	Reynolds number
S	instrument electronic attenuation factor
T	blackbody temperature
V	recorded output voltage
$V_{\lambda 1 bf}$	voltage that would be recorded if flame were a blackbody
α	absorptivity
$\alpha_{\lambda 1 f}$	spectral absorptance of flame
ϵ	emissivity
$\epsilon_{\lambda 1 f}$	spectral emittance of flame
λ	all wavelengths in range of detector and filter
λ_1, λ_2	minimum and maximum detectable wavelengths, respectively
σ	Stefan-Boltzmann constant
$\tau_{\lambda 1 f}$	spectral transmittance such that $1 = \alpha + \tau$.
ϕ	equivalence ratio

Subscripts:

B	burner surface
b	bead
bb	blackbody
c	convective
$f1$	flame radiation only
$f2$	flame radiation plus transmitted blackbody radiation
g	gas
o	blackbody covered with shutter
P	upper plate
r	radiative
s	soot
λ	wavelength
∞	ambient

Appendix B
Program for Calculating Flame Temperature

```
    ∇ X CO2TEMP Y;ALN;AT;EMM;NTBB;NTF;VOLT;NREF;SAT;TAU
[1]  ⍝;TCALC;KSCALC;NDFN;FN
[2]  ⍝ VOLTAGE READING W/O BLACKBODY SOURCE (BBS) = X AND
[3]  ⍝ VOLTAGE READING W/ BLACKBODY = Y
[4]  ⍝ THIS PROGRAM CALCULATES THE SPECTRAL TRANSMITTANCE
[5]  ⍝ (TAU)AND SPECTRAL EMITTANCE OF A FLAME USING THE
[6]  ⍝ 3.94 MICRON INFRARED SPECTROMETER FILTER AND THE
[7]  ⍝ NEUTRAL DENSITY FILTER ND=3
[8]  ⍝ THIS PROGRAM WILL CALCULATE A CALIBRATION CONSTANT
[9]  ⍝ KS,BASED ON THE VOLTAGE READING FOR THE BLACK BODY
[10] ⍝ SOURCE AT 1000 DEGREES C.
[11] ⍝ FOUR READINGS OF VOLTAGE ARE REQUIRED:
[12] ⍝ V[1]=V0,V[2]=VBB,V[3]=VF1,V[4]=VF2
[13]  NTBB←0.051064 ⍝ NT FOR BBS AT 1000 DEGREES C.
[14]  NREF←4.442E¯5 ⍝ NREF FOR CO2 FILTER.
[15]  AT←33 ⍝ CONSTANT ATTENTUATION VALUE.
[16]  SAT←44.6 ⍝ SENSITIVITY FOR ATTENUATION VALUE OF 33.
[17]
[18] ⍝ CALCULATION OF THE CALIBRATION CONSTANT KS FROM THE
[19] ⍝ VOLTAGE READING FOR THE BLACK BODY SOURCE AT 1000 C.
[20]  KSCALC←(SAT×VBB)÷(NTBB-NREF)
[21]  'KSCALC =',(⍕KSCALC)
[22]  VOLT←0,VBB,X,Y
[23]
[24] ⍝ CALCULATE THE SPECTRAL TRANSMITTANCE
[25]  TAU←((VOLT[4]×SAT)-(VOLT[3]×SAT))÷((VOLT[2]×SAT)-
[26]  (VOLT[1]×SAT))
[27]  EMM←1-TAU ⍝ CALCULATE THE EMISSIVITY
[28] ⍝ .964 IS A TRANSMISSION CORRECTION FACTOR, SINCE FLAME
[29] ⍝ IS <60' FROM RAD
[30]  NTF←NREF+((SAT×VOLT[3])÷(KSCALC×EMM×0.964))
[31]  ALN←⍟NTF
[32]  'NTF =',(⍕NTF)
[33]
[34] ⍝  USING A CURVEFIT TO THE NT VS TEMPERATURE TABLE,
[35] ⍝  CALCULATE THE FLAME TEMPERATURE:
[36]  TCALC←6379+(5072.53×ALN)+(2267.85×(ALN*2))+(659.18×
[37]  (ALN*3))+(127.59×(ALN*4))+(16.23×(ALN*5))+(1.295×
[38]  (ALN*6))+(0.0584×(ALN*7))+(1.129E¯3×(ALN*8))
[39]  TCALC←TCALC+273 ⍝ CONVERT TO KELVIN.
[40]  '**************************************************'
[41]
[42] ⍝ PRINT OUT CALCULATED FLAME TEMPERATURE:
[43]  'FLAME TEMPERATURE (DEG. K) =',(⍕TCALC)
    ∇
```

References

1. Santoro, R.J.; Semerjian, H.G.; and Dobbins, R.A.: Soot Particle Measurements in Diffusion Flames. Combust. Flame, vol. 51, no. 2, June 1983, pp. 203–218.
2. Wey, C.: Soot Formation in Gaseous Laminar Diffusion Flames. Ph.D. Thesis, Georgia Institute of Technology, 1984.
3. Prado, G., et al.: Study of Soot Formation in Premixed Propane/Oxygen Flames by In-Situ Optical Techniques and Sampling Probes. Eighteenth Symposium (International) on Combustion, The Combustion Institute, 1981, pp. 1127–1136.
4. Lyons, V.J.: Optical Measurements of Soot in Premixed Flames," Ph.D. Thesis, University of California-Berkeley, 1988.
5. Schmidt, H.: Proof of the Radiation Law in the Case of the Bunsen Flame. Ann. Physik, vol. 29, no. 5, Aug. 10, 1909, pp. 971–1028.
6. Kaskan, W.E.: The Dependence of Flame Temperature on Flame Mass Velocity. Sixth Symposium (International) on Combustion, The Combustion Institute, 1956, pp. 134–143.
7. Kaskan, W.E.: Temperatures of Flames Burning on Porous Burners. Combust. Flame, vol. 4, no. 3, Sept. 1960, pp. 285–288.
8. Toossi, R.: Physical and Chemical Properties of Combustion Generated Soot. LBL–7820, May 1978.
9. Schoenung, S.M.; and Hanson, R.K.: CO and Temperature Measurements in a Flat Flame by Laser Absorption Spectroscopy and Probe Techniques. Combust. Sci. Technol., vol. 24, nos. 5–6, 1981, pp. 227–237.
10. Kaiser, E.W.; Rothschild, W.G.; and Lavoie, G.A.: Effect of Fuel-Air Equivalence Ratio and Temperature on the Structure of Laminar Propane-Air Flames. Combust. Sci. Technol., vol. 33, nos. 1–4, 1983, pp. 123–134.
11. Tourin, R.H.: Monochromatic Radiation Pyrometry of Hot Gases, Plasmas, and Detonations. Temperature—Its Measurement and Control in Science and Industry, Vol. 3, Part 2, Applied Methods and Instruments, A.I. Dahl, ed., Reinhold Publishing Corp., 1962, pp. 455–466.
12. Instruction Manual for Spectral Master Infrared Research Radiometer Model 12-550. Barnes Engineering Company (now Infrared Systems, Inc.), Stamford, CT, 1977.
13. Kiernan, C.L.; Spencer, J.M.; and Turner, J.R.: APL*LUS System, STSC Inc., Rockville, MD, 1985.
14. Ang, J.A., et al.: Temperature and Velocity Profiles in Sooting Free Boundary Layer Flames. AIAA Paper 86–0575, Jan. 1986.
15. Kreith, F.: Principles of Heat Transfer. 3rd ed., Harper & Row, 1973.
16. Jakob, M.: Heat Transfer. Vol. I, John Wiley & Sons, 1949.
17. Siegel, R.; and Howell, J.R.: Thermal Radiation Heat Transfer. McGraw-Hill, 1972.
18. Gordon, S.; and McBride, B.J.: Computer Program for Calculation of Complex Chemical Equilibrium Compositions, Rocket Performance, Incident and Reflected Shocks, and Chapman-Jouguet Detonations. NASA SP–273, 1976.
19. Metghalchi, M.; and Keck, J.C.: Laminar Burning Velocity of Propane-Air Mixtures at High Temperature and Pressure. Combust. Flame, vol. 38, no. 2, June 1980, pp. 143–154.
20. Barnett, H.C.; and Hibbard, R.R., eds.: Basic Considerations in the Combustion of Hydrocarbon Fuels With Air. NACA Report 1300, 1959.

NASA
National Aeronautics and Space Administration

Report Documentation Page

1. Report No.	2. Government Accession No.	3. Recipient's Catalog No.
NASA TP-2900 AVSCOM TR 88-C-008		

4. Title and Subtitle

Determination of Combustion Gas Temperatures by Infrared Radiometry in Sooting and Nonsooting Flames

5. Report Date

February 1989

6. Performing Organization Code

7. Author(s)

Valerie J. Lyons and Carmen M. Gracia-Salcedo

8. Performing Organization Report No.

E-4446

9. Performing Organization Name and Address

NASA Lewis Research Center
Cleveland, Ohio 44135-3191
and
Propulsion Directorate
U.S. Army Aviation Research and Technology Activity—AVSCOM
Cleveland, Ohio 44135-3127

10. Work Unit No.

1L161102AH45
505-62-21

11. Contract or Grant No.

12. Sponsoring Agency Name and Address

National Aeronautics and Space Administration
Washington, D.C. 20546-0001
and
U.S. Army Aviation Systems Command
St. Louis, Mo. 63120-1798

13. Type of Report and Period Covered

Technical Paper

14. Sponsoring Agency Code

15. Supplementary Notes

Valerie J. Lyons, NASA Lewis Research Center; Carmen M. Gracia-Salcedo, Propulsion Directorate, U.S. Army Aviation Research and Technology Activity—AVSCOM.

16. Abstract

Flame temperatures in nonsooting and sooting environments were successfully measured by radiometry for premixed propane-oxygen laminar flames stabilized on a water-cooled, porous sintered-bronze burner. The measured temperatures in the nonsooting flames were compared with fine-wire thermocouple measurements. The results show excellent agreement below 1700 K, and when the thermocouple measurements were corrected for radiation effects, the agreement was good for even higher temperatures. The benefits of radiometry are (1) the flow is not disturbed by an intruding probe, (2) calibration is easily done using a blackbody source, and (3) measurements can be made even with soot present. The theory involved in the radiometry measurements is discussed, as well as the energy balance calculations used to correct the thermocouple temperature measurements.

17. Key Words (Suggested by Author(s))	18. Distribution Statement
Temperature; Flame; Premixed flames; Combustion; Thermocouple; Soot; Radiation; Radiometry; Propane-oxygen flame	Unclassified – Unlimited Subject Category 34

19. Security Classif. (of this report)	20. Security Classif. (of this page)	21. No of pages	22. Price*
Unclassified	Unclassified	14	A03

NASA FORM 1626 OCT 86

*For sale by the National Technical Information Service, Springfield, Virginia 22161

NASA-Langley, 1989